15 December 2000

ELSEVIER

Optics Communications 186 (2000) 329–333

OPTICS COMMUNICATIONS

www.elsevier.com/locate/optcom

A poor man's FROG

C. Radzewicz [a,*], P. Wasylczyk [a], J.S. Krasinski [b]

[a] *Optics Division, Institute of Experimental Physics, Warsaw University, ul. Hoza 69, 00-681 Warsaw, Poland*
[b] *Electrical and Computer Engineering, Center for Laser and Photonics Research, Oklahoma State University, Stillwater, OK 74078 USA*

Received 7 March 2000; received in revised form 7 September 2000; accepted 18 October 2000

Abstract

In this communication we present a new method for recording a two-dimensional second harmonic spectrogram of a femtosecond laser pulse. Filtering of the second harmonic signal due to phase matching in a thick nonlinear crystal is used to spectrally resolve the second harmonic autocorrelation. Amplitude and phase of a pulse can be retrieved from the spectrogram using a standard frequency resolved optical gating iterative algorithm. © 2000 Published by Elsevier Science B.V.

Keywords: Ultrashort laser pulses; Laser pulse characterization; Frequency resolved optical gating

1. Introduction

While we are able to generate shorter and shorter light pulses and femtosecond lasers became available to a wide group of potential users, there is a continuous search for a simple, fast and reliable method capable of characterizing ultrashort laser pulses. There has been much work done in this area in the past, yet out of many different methods proposed [1–5] only two schemes are, at the moment, commonly used for complete amplitude and phase measurement of the pulse electric field.

In a recently introduced spectral phase interferometry for direct electric-field reconstruction (SPIDER) method [6] an interferogram made of two frequency-shifted pulse replicas is recorded. The method requires quite a complex optical set-up and relatively high pulse energies. Its advantage lies in a noniterative, unambiguous and fast numerical procedure used to retrieve the spectral phase from the experimental data.

Frequency resolved optical gating (FROG) method [7] has been introduced about a decade ago and it has been extensively tested since. It is based on measuring spectrally resolved autocorrelation function – a spectrogram. An iterative algorithm [8] retrieves the electric field from the two-dimensional spectrogram. The apparatus here is just an autocorrelator (CW or single shot) with a spectrograph attached to its output. Extremely low-energy pulses can be measured if a second order process is used for the autocorrelation generation but at the cost of time direction ambiguity.

In a typical single-shot second harmonic FROG (SH FROG) set-up, two pulse replicas overlap

* Corresponding author. Tel.: +48-22-625-4738; fax: +48-22-625-4771.

E-mail address: czeslaw.radzewicz@fuw.edu.pl (C. Radzewicz).

0030-4018/00/$ - see front matter © 2000 Published by Elsevier Science B.V.
PII: S0030-4018(00)01077-4

spatially and temporarily in a nonlinear crystal. If the wavefronts intersect at a small angle, different positions along the axis perpendicular to the propagation direction correspond to different delays between the pulses. The second harmonic spatial pattern is imaged onto the spectrometer entrance slit, and the resulting two-dimensional image is recorded with a CCD camera. When femtosecond pulses are to be measured, one necessarily deals with a broad spectrum. Therefore in a standard SH FROG set-up a nonlinear crystal thin enough to provide sufficient bandwidth for second harmonic generation must be used. On the other hand, one can make use of a thick crystal filtering properties to achieve spectral resolution without any additional wavelength-selective device.

2. Intensity autocorrelation function with a thick crystal

Consider a single-shot SH FROG with a type I phase matching in a negative birefringent nonlinear crystal. Two replicas of the measured pulse propagate as ordinary waves while the sum-frequency pulse propagates as an extraordinary wave. We will use the term sum-frequency rather than second harmonic throughout this paper reserving the latter name for frequency- and space-degenerate process. If the crystal is thin enough then phase matching is possible for all the spectral components of the input waves and the signal (sum-frequency) wave E_s is given by

$$E_s(\tau) = \kappa \int_{-\infty}^{+\infty} E(t)E(t+\tau)\,\mathrm{d}t \tag{1}$$

where $E(t)$ is the complex amplitude of the measured pulse, κ is a constant, and the delay τ varies along the direction perpendicular to the propagation direction (Fig. 1a). In such a set-up one measures the spatial distribution of the signal wave intensity which is proportional to the background-free intensity autocorrelation function.

If, however, the crystal is thick then Eq. (1) does not apply because of the bandwidth limitations resulting from phase matching. In a single-shot SH FROG set-up the two input beams propagate at a small angle with respect to each other, and the phase-matching condition is then written in the form: $\boldsymbol{k}(\omega_1) + \boldsymbol{k}(\omega_2) = \boldsymbol{k}(\omega_3)$ (Fig. 1b). For well collimated input beams the directions of the wave vectors $\boldsymbol{k}(\omega_1)$ and $\boldsymbol{k}(\omega_2)$ are fixed. Still, their lengths can vary because of a significant spectral bandwidth of those pulses. If the angle α between the vectors $\boldsymbol{k}(\omega_1)$ and $\boldsymbol{k}(\omega_2)$ is small (the angle in Fig. 1b is strongly exaggerated) and the pulse bandwidth is small compared to the central frequency then, to the first approximation, the direction of $\boldsymbol{k}(\omega_3)$ is also fixed. This noted, one can see that for small values of α the phase-matching condition is approximately the same as that for a collinear sum-frequency generation.

In order to see how the finite bandwidth of the crystal influences the signal measured in a SH FROG set-up we have numerically calculated the efficiency of the collinear sum-frequency generation process in a 3 mm thick KDP crystal. The

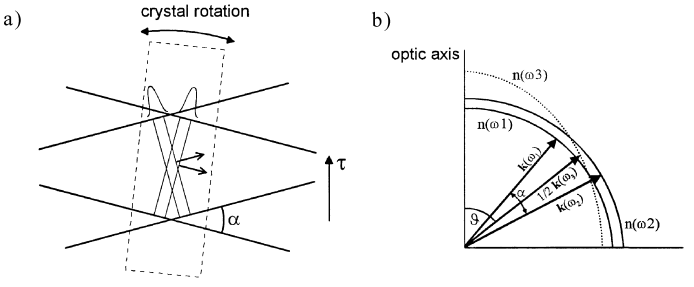

Fig. 1. The idea of the single-shot autocorrelation measurement. (a) Two pulse replicas intersect within a nonlinear crystal (dimensions not to scale). The delay between the pulses varies along the axis perpendicular to the pulse propagation direction. Also shown is the crystal rotation direction for the sum-frequency spectral component selection. (b) Phase-matching condition for type I sum-frequency generation.

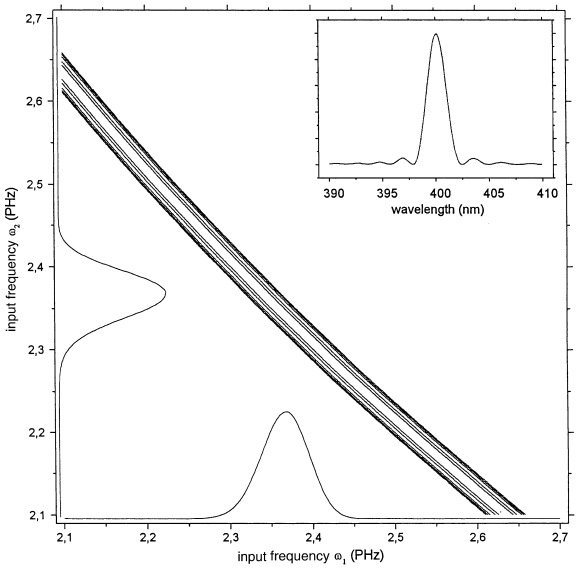

Fig. 2. Calculated normalized efficiency of the collinear sum-frequency generation in a 3 mm thick KDP crystal as a function of two input frequencies. The contours are plotted for the values of 0.05, 0.1, 0.2, 0.5 and 0.75. Laser spectra are displayed on the frequency axes. The inset shows $\omega_1 = \omega_2$ cross-section.

results are shown in Fig. 2. In this figure, the sum-frequency generation efficiency $\eta(\omega_1, \omega_2)$ is plotted versus two input frequencies ω_1 and ω_2. The efficiency is proportional to $\mathrm{sinc}^2(x)$ with x defined as $x = [\boldsymbol{k}(\omega_1) + \boldsymbol{k}(\omega_2) - \boldsymbol{k}(\omega_3)]L/2$, where $\boldsymbol{k}(\omega_i)$ is the magnitude of the wave vector for the ith wave, L is the crystal thickness and the energy conservation condition defines ω_3: $\omega_3 = \omega_1 + \omega_2$. In the coordinate system shown in the figure, fixed output frequencies ($\omega_3 = \mathrm{const}$) correspond to straight lines at $-45°$ with respect to ω_1 axis. This feature can be used to estimate the bandwidth of the sum-frequency generation process in the following way. Tuning a single frequency input corresponds to moving along the line $\omega_1 = \omega_2$ on the ω_1, ω_2 plane. In this case only a finite-width range of input frequencies can be efficiently converted into the sum-frequency wave and, consequently, the range of output frequencies is also limited. Similar bandwidth limitations will be imposed on the output in the case of broadband input pulses, however any pair of input frequencies ω_1 and ω_2 can be efficiently converted as long as the sum $\omega_1 + \omega_2$ stays within the window defined by the crystal phase-matching properties. For the particular case studied here (a 3 mm KDP crystal and frequencies corresponding to 700–900 nm wavelength range) the constant intensity contours can be very well approximated by straight lines at $-45°$ with respect to ω_1 axis.

This result can be understood as follows. The two input waves can drive nonlinear polarization in the crystal at any frequency allowed by their bandwidths; however, only a limited range of spectral components of this polarization is favoured by phase-matching condition. To calculate the spectral width of the output wave in the case of broadband input waves one should make a projection of $\eta(\omega_1, \omega_2)$ onto a plane perpendicular to the ω_1, ω_2 plane and containing $\omega_1 = \omega_2$ line. In our particular case an almost identical result is obtained by taking a cross-section of $\eta(\omega_1, \omega_2)$ along $\omega_1 = \omega_2$ line. Such a cross-section is shown in the inset in Fig. 2. This curve can be used to estimate the width of the spectral window due to the application of a thick SHG crystal, which for our 3 mm KDP is approximately 2 nm FWHM.

The choice of the crystal thickness is limited, on one hand, by the desired spectral resolution and, on the other hand, by the crystal dispersion. The spectral resolution increases with the crystal thickness but so does the pulse distortion due to group velocity dispersion. To estimate the pulse broadening we have calculated that for the 3 mm KDP crystal considered here, a 30 fs (FWHM), 800-nm-centred Fourier limited pulse is stretched to approximately 31 fs after propagation through the crystal. For our diagnostic applications, such distortion is still at the acceptable level. The calculations for BBO, $LiIO_3$ and KDP show that for crystal thickness leading to the above pulse broadening the spectral resolution is almost the same. Thus, the choice of nonlinear crystal is not critical in our method.

To conclude this section, using a nonlinear crystal with properly chosen thickness in a non-collinear second harmonic autocorrelator is equivalent to using a system containing a thin nonlinear crystal and a spectral filter acting on the output wave, i.e. a system required for SH FROG measurements.

3. Experiment and results

To characterize pulses from a home-built femtosecond Kerr lens mode-locked Ti:Al_2O_3 laser, we have built a standard single-shot autocorrelator with a 3 mm thick KDP crystal. Second harmonic intensity spatial distribution in the crystal output surface is imaged onto a 1 in. 1024 element linear CCD detector. The crystal can be rotated around the axis perpendicular to the laser beams' propagation direction, and each angular position corresponds to effective second harmonic generation within a certain wavelength range and therefore to a specific spectral component of the autocorrelation function. The autocorrelations measured for different angles are then combined to give a two-dimensional wavelength-delay spectrogram.

To calibrate the system, the spectra of the autocorrelation function were recorded for different angles of crystal rotation, and the position of the maximum was measured for each spectrum. The results are presented in Fig. 3. The 'spectral resolution' determined by the spectra's width is a free parameter that can be set by appropriate choice of the nonlinear crystal and its thickness. With a 3 mm thick KDP crystal, the resolution is approximately 2 nm at 800 nm which is consistent with results presented in the previous section. This resolution is worse than that of a good spectrometer but still sufficient for our purposes. As the FROG algorithms use equal spacing on the wavelength axis, the linear angle-wavelength dependence was assumed, a good approximation for small angle range used in the experiment. The spectral calibration has to be done only once. Once recorded, it can be used in all the subsequent measurements.

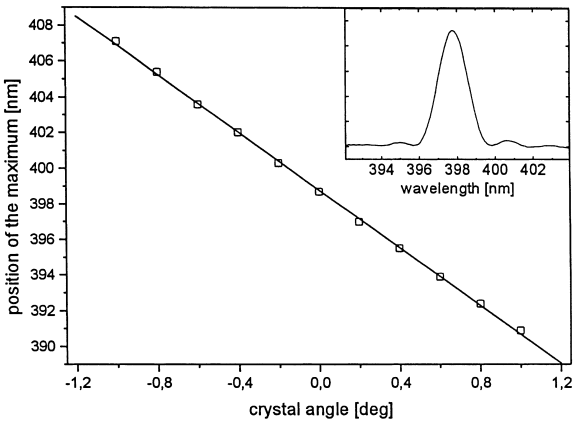

Fig. 3. Wavelength of the second harmonic spectrum maxima versus crystal angular position with a fitted linear dependence. One of the SH spectra is shown in the insert. The spectrum width FWHM is approximately 2 nm.

The temporal calibration of the autocorrelator was performed in a standard way by introducing a known delay into one of the input beams and measuring the spatial shift of the autocorrelation trace.

To characterize laser pulses, a set of 15 autocorrelations was recorded for different crystal angles ranging from $-1.4°$ to $+1.4°$ around an arbitrarily chosen 'zero' position in steps of 0.2°. We arranged the autocorrelations, each consisting of 63 points, as columns of a 15×63 matrix. From this matrix the spectral amplitude and phase was retrieved using a standard iterative FROG algorithm running on PC. The results are shown in Fig. 4.

The Ti:sapphire laser was initially set to get reasonably short pulses with a standard CW autocorrelator. Still, as one can see in Fig. 4, there is a significant quadratic component present in the spectral phase. This is consistent with the fact that the pulse duration FWHM (approximately 50 fs) is 1.6 times the transform limit. As a simple consistency check, we verified first that the spectral amplitude retrieved with our method is in a good

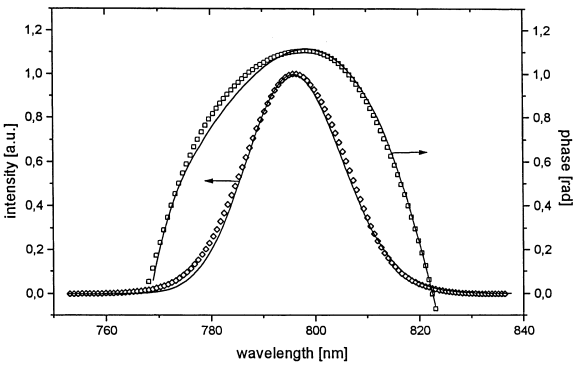

Fig. 4. Spectral amplitude and phase for pulses from a femtosecond Ti:sapphire laser obtained with a standard FROG method (—) and a poor man's FROG method (◇ and □).

agreement with the laser spectrum which was measured independently with a spectrometer.

As we have mentioned in the previous section, using a thick nonlinear crystals can result in some distortion of the input pulses as they propagate in a dispersive medium because of the group velocity dispersion. This in turn could distort the FROG spectrogram leading to errors in the retrieved spectral amplitude and phase. In order to check whether this effect is significant in our experiment we have used a standard SH FROG set-up with a 200 μm thick KDP crystal and 150 mm imaging spectrometer to characterize the pulses from our Ti:sapphire oscillator. Fig. 4 shows the comparison between the spectral amplitude and phase of the laser pulses retrieved from a standard SH FROG and a poor man's FROG. The FROG error [9] was 0.0019 for poor man's FROG compared to 0.00079 for the standard FROG. As one can see the overall agreement between the results obtained with the two methods is very good. The spectral amplitudes agree to within a few percent while the spectral phases are the same with accuracy better than 0.06 rad over the whole spectrum. We conclude from those results that, in our experiment, the group velocity dispersion effects due to the thick nonlinear crystal are not very important and do not lead to appreciable errors in the results.

4. Conclusions

In conclusion, we have demonstrated a new, simple method which allows to record spectrally resolved second harmonic autocorrelation function of femtosecond laser pulses in a very simple and inexpensive experimental set-up. The method relies on spectral filtering introduced by a thick nonlinear crystal. To our best knowledge, the system presented in this paper is the simplest and least expensive apparatus capable of full diagnostics of femtosecond laser pulses.

The amplitude and phase of 50 fs pulses from a Ti:sapphire laser were retrieved from two-dimensional experimental data using a standard FROG iterative algorithm. We have compared the results obtained from our method with those from a standard SH FROG and found a very good agreement indicating that our method indeed returns correct values of spectral amplitude and phase of femtosecond laser pulses.

Acknowledgements

This work was supported by KBN, grant number 2 P03B 019 18. Also, support of this project by OSU CLPR is appreciated.

References

[1] J.-C.M. Diels, J.J. Fontaine, I. McMichael, F. Simoni, Appl. Opt. 24 (1985) 1270.
[2] J.L.A. Chilla, O.E. Martinez, Opt. Lett. 16 (1991) 39.
[3] K.C. Chu, J.P. Heritage, R.S. Grant, K.X. Xiu, A. Dienes, Opt. Lett. 20 (1995) 904.
[4] E.T.J. Nibbering, M.A. Franco, B.S. Prade, G. Grillon, J.-P. Chambaret, A. Mysyrowicz, J. Opt. Soc. Am. B 13 (1996) 317.
[5] A. Baltuska, Z. Wei, E.T.J. Nibbering, M.A. Franco, A. Mysyrowicz, Appl. Phys. B 65 (1997) 175.
[6] C. Iaconis, I.A. Walmsley, IEEE J. Quant. Electron. 35 (1999) 501.
[7] D.J. Kane, R. Trebino, IEEE J. Quant. Electron. 29 (1993) 571.
[8] K.W. DeLong, R. Trebino, J. Opt. Soc. Am. A 11 (1994) 2429.
[9] R. Trebino, D.J. Kane, J. Opt. Soc. Am. A 10 (1993) 1101.